

Co-pyrolysis of corn stover and waste tire: Pyrolysis behavior and kinetic study based on Fraser-Suzuki deconvolution procedure

Guanqun Luo^{a,b}, Weimin Wang^{a,b}, Wen Xie^c, Yuanjun Tang^b, Yousheng Xu^b, Kaige Wang^{c,*}

^a Cryogenic Center, Zhejiang University City College, Hangzhou 310015, China

^b Department of Energy and Environment System Engineering, Zhejiang University of Science and Technology, Hangzhou 310023, China

^c State Key Laboratory of Clean Energy Utilization, Zhejiang University, Hangzhou 310027, China

ARTICLE INFO

Keywords:

Co-pyrolysis

Biomass

Waste tire

Kinetics

Fraser-Suzuki deconvolution

ABSTRACT

Co-pyrolysis of biomass with waste tire, a hydrogen-rich material, can both improve the quality of bio-oil and mitigate the environmental issue caused by the disposal of waste tires. In this study, co-pyrolysis of corn stover and waste tire was firstly performed in a micro pyrolyzer, and positive synergistic effects were observed, promoting the production of hydrocarbon compounds. Additionally, the kinetics of co-pyrolysis of corn stover and waste tire were investigated. Due to the complexities of the co-pyrolysis process, the global process was divided into reactions of seven pseudo-components using the Fraser-Suzuki deconvolution function. The deconvolution results presented a good fit with experimental results. The activation energy of each pseudo-component was calculated using Kissinger-Akahira-Sunose (KAS), Flynn-Wall-Ozawa (FWO), and Friedman methods. Activation energy of each pseudo-component calculated from above mentioned methods did not greatly varied. Pseudo-component additives in waste tire with low thermal stability had the lowest activation energy (118.21–127.10 kJ/mol), and lignin in corn stover and synthetic rubbers (SR) in waste tire showed high activation energies since they are more thermally stable. The reaction mechanism was then determined using the master plot method. The results of the study are expected to provide more accurate basic information for further scale-up of the co-pyrolysis process.

1. Introduction

Current overwhelming reliance on fossil fuels is the primary cause of climate change, posing increasingly severe risks for ecosystems and human health. The world thus needs a rapid transition away from fossil fuels towards clean and renewable energy to eliminate these risks and achieve a sustainable future for the planet. Biomass with an annual global production of 220 billion dry tons is considered as one of the most promising renewable energy sources to replace fossil fuels [1]. It is predicted that biomass energy would contribute approximately 15–50% of the global primary energy consumption in 2050 [2]. Among different biomass to energy conversion technologies, fast pyrolysis (a rapid thermal decomposition of organic matter in the absence of oxygen) has attracted more interests for production of liquid fuels with advantages of easy storage and transport.

Bio-oil as the major product from fast pyrolysis of biomass usually has high oxygen and water content, high corrosiveness, and low heating value, limiting its direct application [1,3,4]. These detrimental

properties are mainly caused by the low H/C_{eff} ratio of biomass (< 0.3) [5,6]. Co-pyrolyzing biomass with high H/C_{eff} ratio reactants has been proposed as a promising method to improve the quality of raw bio-oil⁷. Waste tire is characterized as low ash content, high volatile content, and relatively high H/C_{eff} ratio (~0.8), making them ideal co-feeding reactants for biomass pyrolysis [7,8]. Niu et al. [9] studied co-pyrolysis of moso bamboo and waste tire in a fixed bed reactor, and found that addition of waste tire increased production of bio-oil and decreased oxygen content in bio-oil. Farooq et al. [10] also reported positive synergistic effects when investigated the co-pyrolysis of wheat straw and waste tire. Compared to the bio-oil from pyrolysis of wheat straw, bio-oil from co-pyrolysis was more stable with lower oxygen content, higher carbon and hydrogen content, and thus higher heating value. Similar results were also obtained by Martinez et al. [11] and Cao et al. [12]. Roughly 17 million tons of waste tire are produced worldwide yearly, and disposal of these waste tire is a challenging task because of their high durability, non-biodegradability, and complex compositions [13, 14]. Waste tire is traditionally disposed of in landfills or in stockpiles,

* Corresponding author.

E-mail address: kaigewang@zju.edu.cn (K. Wang).

<https://doi.org/10.1016/j.jaap.2022.105743>

Received 19 July 2022; Received in revised form 26 September 2022; Accepted 27 September 2022

Available online 17 October 2022

0165-2370/© 2022 Elsevier B.V. All rights reserved.

consuming valued space. Combustion of waste tire may also produce toxic air pollutants [15]. Thus, usage of waste tire as hydrogen donor in biomass pyrolysis process cannot only improve bio-oil quality, but recapture energy and mitigate waste management problems [16].

Understanding the kinetic features is of great importance to design, optimize, and scale up the co-pyrolysis process of biomass and waste tire. Thermogravimetric analysis (TGA) has been proven as a powerful tool to investigate the pyrolysis kinetics. Model-free method combined with isoconversional method has been extensively applied to the data obtained from TGA to estimate kinetic parameters of biomass and waste tire co-pyrolysis process, because this method can be utilized without knowing the pyrolysis mechanism (model) [17]. Söyler and Ceylan [18] performed the kinetic analysis of hazelnut shell and waste tire co-pyrolysis using model-free Straink, and Flynn-Wall-Ozawa (FWO) methods, and found that the activation energy of co-pyrolysis was higher than pyrolysis of hazelnut shell or waste tire alone. Rasam et al. [19] applied different isoconversional methods including FWO, Kissinger-Akahira-Sunose (KAS), Starink (STK), and Vyazovkin (VYA) to study the kinetics of pyrolysis of microalgae, bagasse, scrap tire, and their binary and ternary mixtures. Activation energies calculated by these methods were similar. For binary mixtures pyrolysis, pyrolysis of microalgae and bagasse had the lowest activation energy, and the addition of scrap tire increased activation energy of ternary mixtures pyrolysis. Similar results were also obtained by Azizi et al. [20] when investigating the kinetic behaviors of pyrolysis of microalgae *Chlorella vulgaris*, wood, scrap tire, and their blends using FWO and KAS methods. The studies mentioned above all considered the pyrolysis process as a global process (single-step mechanism) to conduct the kinetic analysis, which over simplified the actual reaction processes and may cause inaccurate estimations of kinetic parameters.

Lignocellulosic biomass is a complex biopolymer mainly composed of hemicellulose, cellulose, and lignin, and therefore the chemical reactions involved in its pyrolysis process are very complex, consisting of a set of competitive, parallel, and sequential reactions [21]. The three-parallel-reaction model combined with model-free method (multi-step mechanism), in which pyrolysis of lignocellulosic biomass is separated into three reactions of each pseudo-component (i.e. hemicellulose, cellulose, and lignin), has been proven to be more suitable to precisely estimate the kinetic parameters of lignocellulosic biomass pyrolysis process [22–24]. Hu et al. [22] studied pyrolysis kinetics of three types of lignocellulosic biomass (i.e. pine wood, rice husk, and bamboo) using three-parallel-model, separating the global process into reactions of three pseudo-components (i.e. hemicellulose, cellulose, and lignin). Activation energies of three pseudo-components were determined by Friedman method. For pyrolysis of all three feedstock, activation energies of their three pseudo-components varied slightly with conversion rates, indicating that multi-step mechanism is an appropriate approach to accurately estimate pyrolysis kinetic parameters. Like biomass, tire is also a complex polymer and a series of complex reactions are simultaneously occurring and overlapping during its pyrolysis process. Therefore, multi-step mechanism has been widely applied to analyze the kinetic behaviors of tires [13,25–28]. Leung et al. [25] studied the kinetics of scrap tire pyrolysis using two types of multi-step methods (i.e. three-component-simulation model and three-elastomer simulation model) followed by Coats-Redfern method. In the three-component model, tire pyrolysis was treated as the sum of three major degradable components pyrolysis processes, while tire pyrolysis was separated into three reactions of natural rubber (NR), butadiene rubber (BR), and styrene-butadiene rubbers (SBR) in the three-elastomer model. Both simulations matched well with experimental data. Lopez et al. [29] studied the effect of vacuum on the tire pyrolysis kinetics, and separated the pyrolysis process into three pseudo-reactions of tire major components (i.e. volatiles, NR, and SBR). Results showed that activation energy of each pseudo-component decreased under vacuum.

Unfortunately, limited research on kinetics of co-pyrolysis biomass and hydrogen donor using multi-step mechanism has been reported to

date. Wang et al. [30], Ephraim et al. [31], and Wen et al. [32] analyzed the kinetic behaviors of co-pyrolysis of lignocellulosic biomass and plastics via deconvolution procedure. To the best of our knowledge, there are no studies so far applied multi-step mechanism to analyze the kinetic features of co-pyrolysis of lignocellulosic biomass and waste tire. In this work, pyrolysis characteristics and kinetic features of co-pyrolysis of corn stover and waste tire were investigated. For kinetic study, multi-step method was applied. The overall reaction was first separated into several pseudo-reactions using Fraser-Suzuki deconvolution method. The activation energy of each pseudo-reaction was then estimated using Friedman, KAS, and FWO isoconversional methods, and master plots method was used to determine the suitable reaction model for the degradation of each pseudo-component. This work aims to provide more precise fundamental information for further development of co-pyrolysis process of lignocellulosic biomass and waste tire.

2. Materials and methods

2.1. Materials

The feedstock used in this work are corn stover and waste tire. Corn stover was purchased from a farm in Suqian city, Jiangsu Province, China. Corn stover feedstock was ground and sieved into a particle size of less than 80 mesh. Waste tire powder (~80 mesh) was purchased from a tire recycling company in Shanxi Province, China. The ultimate and analysis proximate results of them are shown in Table 1.

2.2. Fast pyrolysis

A furnace-type pyrolyzer (Py, 2020iD, Frontier Laboratories, Japan) was used for the fast pyrolysis experiments. Approximately 0.5 mg feedstock was put into the sample cup. For co-pyrolysis, the mass ratio of corn stover and waste tire was 1: 1. The sample cup was then dropped into the preheated pyrolysis reactor. Pyrolysis temperature was set at 500 °C, and the interface temperature was kept at 300 °C to prevent the product condensation. Helium with a flow rate of 100 mL/min was used as carrier gas to sweep the pyrolysis vapors into a downstream gas chromatograph (GC, 8860, Agilent Technologies, USA) for analysis.

The GC was equipped with a three-way splitter that directed the pyrolysis vapor stream into three detectors, namely a mass spectrometer (MS, 5977B, Agilent Technologies, USA), a flame ionization detector (FID) and a thermal conductivity detector (TCD). The GC column was a HP-5 capillary column (30 m × 0.32 mm I.D. × 0.25 mm film thickness), and the GC oven was programmed for a 3 min hold at 40 °C, and then ramped at 5 °C/min to 300 °C, after which temperature was held constant for 10 min. Pyrolysis volatiles were identified by comparing with the NIST mass spectral library and the retention time of the known standards. Additionally, semi-quantitative analysis of pyrolysis volatiles was performed by recording the peak area percentage to represent the concentration of the identified compounds. Replicates were conducted in this study to confirm the reproducibility of the experiments.

Table 1
Ultimate and proximate analysis of corn stover and waste tire.

Sample	Corn stover	Waste tire
Ultimate analysis (wt%)		
C	34.78	72.62
H	4.27	5.94
O	59.19	18.84
N	1.76	0.85
S	0	1.75
Proximate analysis (wt%)		
Moisture	4.52	0.63
Volatiles	59.09	62.51
Fixed carbon	23.63	27.18
Ash	12.75	9.68

2.3. Thermogravimetric analysis

Pyrolysis of corn stover, waste tire, and their mixtures was conducted using a TGA/DSC 3 + analyzer (Mettler Toledo Corporation, Switzerland) at different heating rates (i.e. 5, 10 and 20 °C/min). For each experiment, about 10 mg oven-dry sample was pyrolyzed under an inert nitrogen atmosphere from room temperature to 800 °C. The nitrogen flow rate was 100 mL/min. For co-pyrolysis experiment, corn stover and waste tire powders were well mixed with a mass ratio of 1: 1.

2.4. Kinetic study

The reaction rate of pyrolysis process can be expressed as:

$$\frac{d\alpha}{dt} = k(T)f(\alpha) \quad (1)$$

t is the reaction time (min). $f(\alpha)$ denotes the differential form of reaction mechanism function, depending on the degree of conversion, α . α is defined as:

$$\alpha = \frac{m_0 - m_t}{m_0 - m_f} \quad (2)$$

where m_0 and m_f represent initial and final sample mass (mg), and m_t denotes the sample mass (mg) at a given time t .

$k(T)$ is the temperature-dependent rate constant. According to the Arrhenius equation, $k(T)$ can be expressed as:

$$k(T) = A \exp\left(\frac{-E}{RT}\right) \quad (3)$$

where T is the absolute temperature (K), A is pre-exponential factor (s^{-1}), E is apparent activation energy (kJ mol^{-1}), and R is the gas constant ($8.3145 \text{ J mol}^{-1} \text{ K}^{-1}$).

Substituting Eq. (3) into Eq. (1) gives:

$$\frac{d\alpha}{dt} = A \exp\left(\frac{-E}{RT}\right) f(\alpha) \quad (4)$$

In the TGA experiments, samples were heated at a constant heating rate β ,

$$\beta = \frac{dT}{dt} = \frac{dT}{d\alpha} \cdot \frac{d\alpha}{dt} \quad (5)$$

Combining Eq. (5) into Eq. (4) gives:

$$\frac{d\alpha}{dT} = \left(\frac{A}{\beta}\right) \exp\left(\frac{-E}{RT}\right) f(\alpha) \quad (6)$$

2.4.1. Fraser-Suzuki deconvolution method

The global derivative thermogravimetric (DTG) curves were deconvoluted into curves of several pseudo-components using asymmetrical Fraser-Suzuki function in this study. Fraser-Suzuki function is given in equation:

$$\frac{d\alpha}{dT} = \sum_{i=1}^{N_c} C_i H_{p,i} \exp\left\{-\frac{\ln 2}{A_{s,i}^2} \ln\left[1 + 2A_{s,i} \frac{(T - T_{p,i})}{W_{hf,i}}\right]^2\right\} \quad (7)$$

where N_c is the total number of pseudo-components, C_i is the proportion of i^{th} pseudo-component, and H_p , W_{hf} , T_p and A_s denotes respectively the maximum peak height (K^{-1}), peak half-width (K), peak temperature (K), and asymmetry (dimensionless) of the $d\alpha/dT$ versus T profile for the i^{th} pseudo-component. The unknown parameters in Eq. (7) were initially guessed and then adjusted by minimizing the deviations $Dev(\%)$ between calculated and experimental values. Nonlinear least squares method was used to calculate $Dev(\%)$:

$$Dev(\%) = \frac{\sqrt{\left(\sum_{j=1}^{N_d} \left[\left(\frac{d\alpha}{dT}\right)_{j,c} - \left(\frac{d\alpha}{dT}\right)_{j,e}\right]^2\right) / N_d}}{h} \times 100 \quad (8)$$

where N_d is the total number of data points, subscript j is referred to j^{th} experimental data point, h is the maximum value of $d\alpha/dT$, and $(d\alpha/dT)_{j,e}$ and $(d\alpha/dT)_{j,c}$ denote the calculated (sum of all the deconvolution peaks) and experimental DTG data, respectively.

2.4.2. Estimation of apparent activation energy

The apparent activation energies of each pseudo-component were estimated by three isoconversional methods including Friedman, KAS, and FWO methods.

The Friedman method is the differential based isoconversional approach, which can be expressed as:

$$\ln\left(\frac{d\alpha}{dT}\right)_{\alpha,i} = \ln\left[\beta_i \left(\frac{d\alpha}{dT}\right)_{\alpha}\right] = \ln[A_{\alpha} f(\alpha)] - \frac{E_{\alpha}}{RT_{\alpha,i}} \quad (9)$$

The integral arrangement of Eq. (4) gives:

$$g(\alpha) = \int_0^{\alpha} \frac{1}{f(\alpha)} d\alpha = \frac{A}{\beta} \int_{T_0}^T \exp\left(\frac{-E}{RT}\right) dT \quad (10)$$

in which $g(\alpha)$ is the integral form of $f(\alpha)$. Table S1 shows the most common $f(\alpha)$ functions and corresponding $g(\alpha)$ functions.

KAS is one of the versatile integral isoconversional method, linearising Eq. (10) can obtain its expression:

$$\ln\left(\frac{\beta_i}{T_{\alpha,i}^2}\right) = \ln\left(\frac{A_{\alpha} R}{E_{\alpha} g(\alpha)}\right) - \frac{E_{\alpha}}{RT_{\alpha,i}} \quad (11)$$

FWO is also an integral form isoconversional method. Linearising Eq. (10) acquires the following expression:

$$\ln(\beta_i) = \ln\left[\frac{A_{\alpha} E_{\alpha}}{R g(\alpha)}\right] - 5.331 - 1.052 \left(\frac{E_{\alpha}}{RT_{\alpha,i}}\right) \quad (12)$$

$T_{\alpha,i}$ in Eqs. (9), (11), and (12) is the temperature corresponding to the given conversion α at i^{th} heating rate. For Friedman, KAS, and FWO methods, graphs of $\ln[\beta_i (d\alpha/dT)_{\alpha}]$ versus $1000/T_{\alpha}$, $\ln[\beta_i / T_{\alpha}^2]$ versus $1000/T_{\alpha}$, $\ln(\beta_i)$ versus $1000/T_{\alpha}$ were respectively plotted, and the apparent activation energy was estimated based on the slopes ($-E_{\alpha}/R$).

2.4.3. Determination of reaction model and pre-exponential factor

The reaction model $f(\alpha)$ of co-pyrolysis of each pseudo-component was determined using Malek master plots method[33].

$$\frac{Y(\alpha)}{Y(0.5)} = \frac{f(\alpha)g(\alpha)}{f(0.5)g(0.5)} = \left(\frac{T}{T_{0.5}}\right)^2 \frac{\left(\frac{d\alpha}{dt}\right)}{\left(\frac{d\alpha}{dt}\right)_{0.5}} \quad (13)$$

where $T_{0.5}$ and $(d\alpha/dt)_{0.5}$ are the temperature and reaction rate at $\alpha = 0.5$, respectively. The graph between $\frac{f(\alpha)g(\alpha)}{f(0.5)g(0.5)}$ (presented in Table S1) versus α gives the theoretical master plots, while $\left(\frac{T}{T_{0.5}}\right)^2 \frac{\left(\frac{d\alpha}{dt}\right)}{\left(\frac{d\alpha}{dt}\right)_{0.5}}$ versus α gives the experimental plot. The most suitable reaction model $f(\alpha)$ was selected as the experimental plot best matches the theoretical master plots. Bringing the determined activation energy and reaction mechanism $f(\alpha)$ into Eq. (4), the value of pre-exponential factor can be calculated.

3. Results and discussion

3.1. Fast pyrolysis in Py-GC/MS

Fast pyrolysis of corn stover, waste tire, and their mixtures at 500 °C was conducted using Py-GC/MS, producing a broad range of volatile products, which can be classified into hydrocarbons, oxygenates, and other N-containing and S-containing compounds (Tables S2–S4). Fig. 1 shows the product distribution for individual fast pyrolysis of corn stover and waste tire, and co-pyrolysis of them at mixing ratio of 1: 1. The major products from fast pyrolysis of corn stover were oxygenate compounds (66.11%) including alcohols, phenols, acids, furans, and carbonyls, followed by hydrocarbons (32.72%). Hydrocarbon species were mainly olefins (29.72%) and alkanes (2.99%). No aromatic compounds were detected. Adding 50 wt% waste tire into biomass feedstock significantly increased the production of hydrocarbons to 81.93%, while decreased the production of oxygenates to 16.53%. For hydrocarbon products, olefins were the dominant components (69.58%) followed by alkanes (7.00%) and aromatics (5.43%). Fast pyrolysis of waste tire mainly produced hydrocarbons (84.91%), among which alkanes, olefins, and aromatics respectively contributed 6.9%, 73.7%, and 4.31%. D-limonene (27.93%) and isoprene (23.22%) were the two major olefinic products. D-limonene was primarily generated by breaking and intramolecular cyclization of NR, which is a versatile chemical and could be widely used in the field of medicine, industry, and agriculture[34].

To further quantitatively depict the synergistic effects on product distributions for co-pyrolysis of corn stover and waste tire, the peak area percentage difference between experimental and theoretical values ΔA was defined:

$$\Delta A = A_{Exp} - A_{Cal} = A_{Exp} - (k_1 A_1 + k_2 A_2) \quad (14)$$

where A_{Exp} and A_{Cal} represent the peak area percentage of corresponding products obtained from experiment and theoretical calculation. A_1 and A_2 denote the peak area percentage of corresponding products from individual pyrolysis of corn stover and waste tire, and $k_1 = k_2 = 0.5$, representing the initial mass fractions of corn stover and waste tire feedstocks in co-pyrolysis processes.

Fig. 2 presents the experimental and theoretical product distribution for co-pyrolysis and variations between experimental and theoretical values. For hydrocarbon production, experimental value was higher than theoretical value with $\Delta A = 23.12\%$, indicating a promoting effect on hydrocarbon production took place during co-pyrolysis. In the contrast, in term of oxygenates production, the experimental value was lower than the theoretical value with $\Delta A = -22.63\%$, implying an inhibiting effect on producing oxygenate compounds in co-pyrolysis

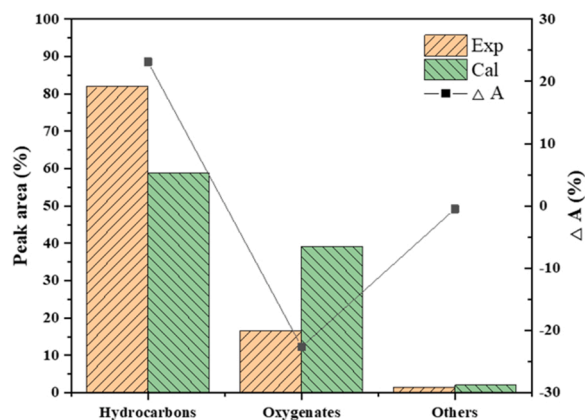


Fig. 2. Experimental and theoretical product distribution for co-pyrolysis and variations between experimental and theoretical values.

process. Similar results were obtained by Wang et al. when studied the co-pyrolysis of biomass (i.e. rice straw and poplar wood) and waste tire [35]. During co-pyrolysis, waste tire as a hydrogen donor had a great impact on the product distribution. Increasing addition of waste tire into biomass promoted the production of hydrocarbons in fast pyrolysis[35].

The reaction process of co-pyrolysis of corn stover and waste tires can be described by a free radical mechanism. Water and light volatile fractions in corn stover and waste tire samples evaporate first after heat exposure. As the temperature further increases, the breakage of oxygen-containing functional group bonds in corn stover takes place, releasing free radicals that can promote the chain breakage of some components in waste tire such as polyisoprene and polystyrene-butadiene[35,36]. The hydrogen radicals released from the waste tire can also interact with the oxygenated components generated by the pyrolysis of corn stover and promote their conversion to hydrocarbon products through hydrogen transfer reactions[3,37]. The possible reaction pathway is shown in Fig. 3.

3.2. Thermogravimetric analysis

Fig. 4(a) showed the TG and DTG profiles of pyrolysis of corn stover at heating rates of 5, 10, and 20 °C/min. The decomposition of corn stover occurred in two regions. The first region took place before 150 °C with little weight loss of 4.68%, mainly attributed to the removal of moisture and light volatiles in corn stover. The significant mass loss (59.58%) occurred in the second region (> 150 °C), which corresponds

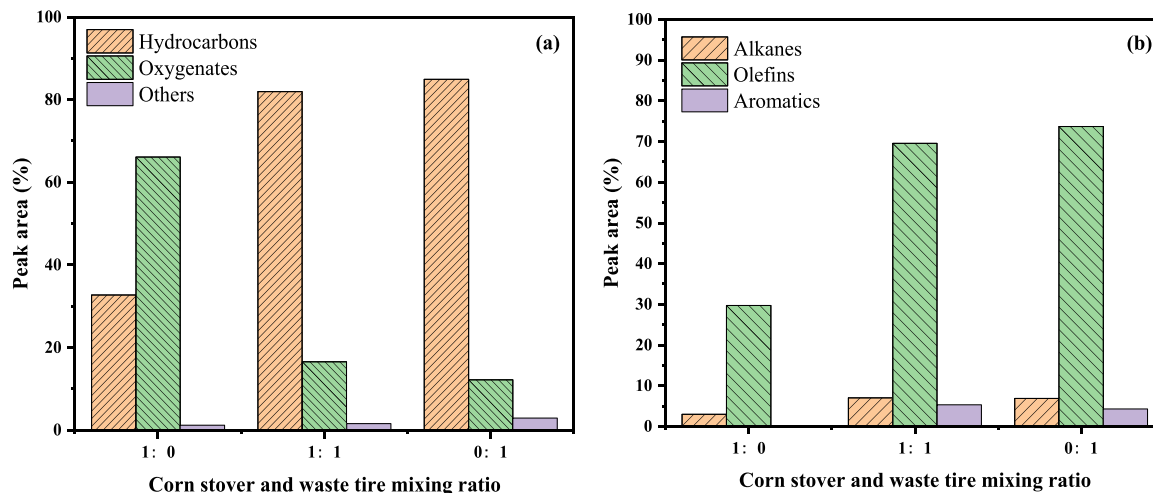


Fig. 1. Product distribution for pyrolysis/co-pyrolysis of corn stover and waste tire: (a) total volatile products and (b) hydrocarbon products.

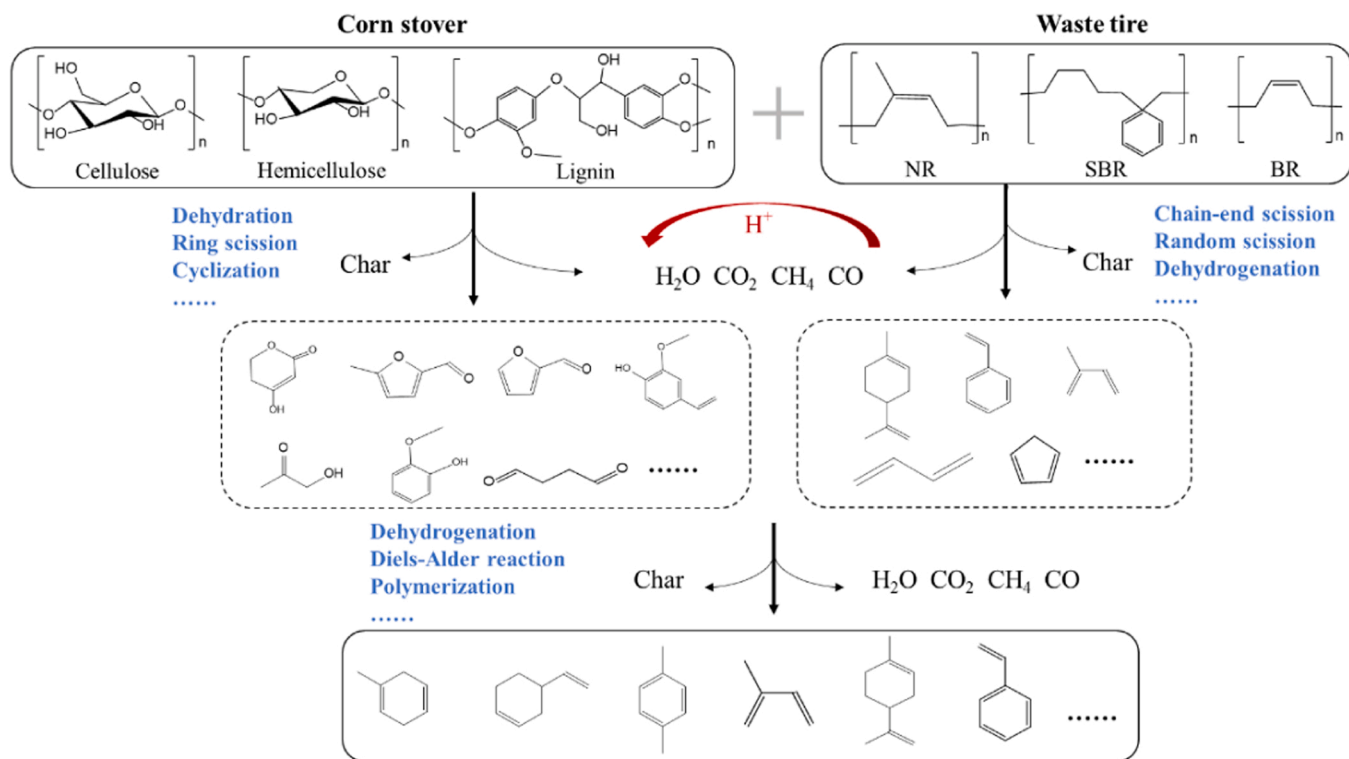


Fig. 3. Proposed reaction pathway for co-pyrolysis of corn stover and waste tire.

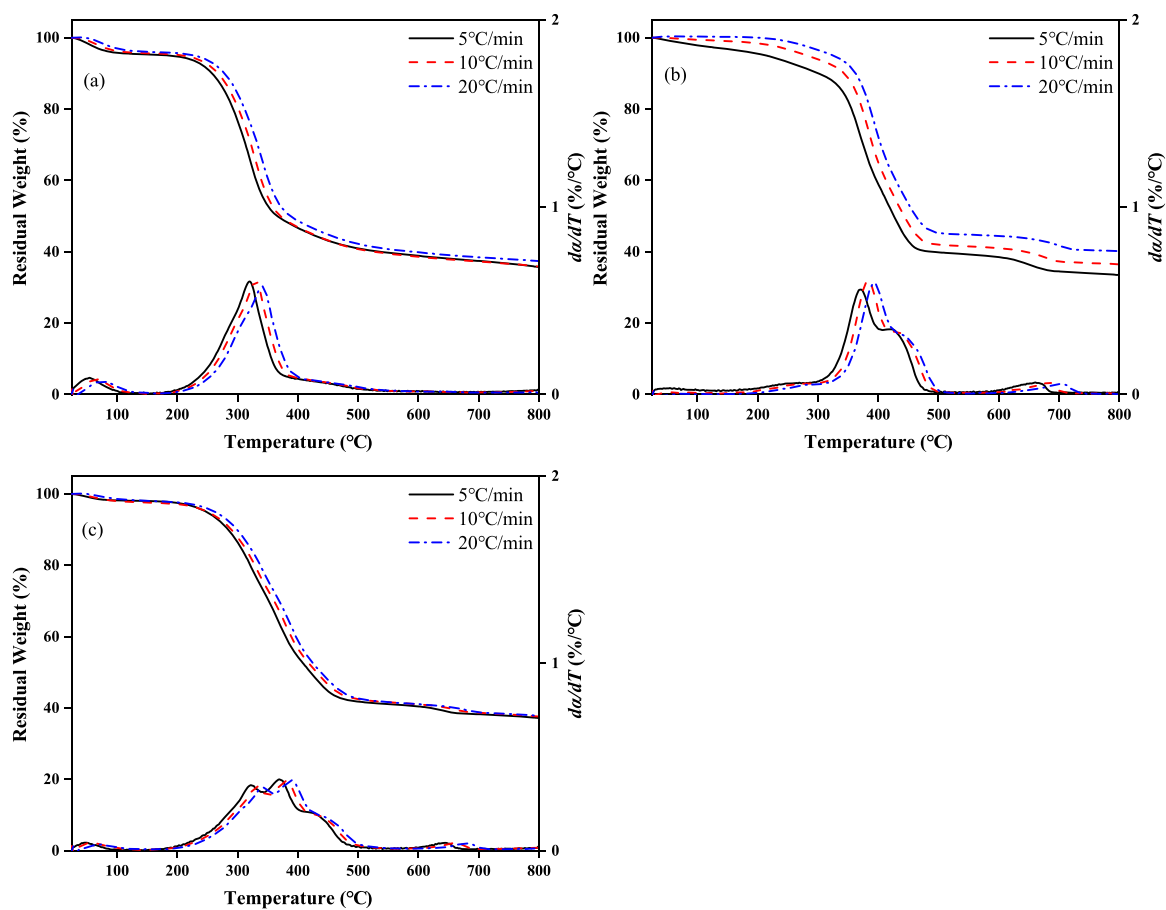


Fig. 4. TG and DTG profiles of feedstock at heating rates of 5, 10, and 20 °C/min: (a) corn stover; (b) waste tire; (c) corn stover and waste tire mixtures.

to the release of volatile matters in corn stover. Corn stover is classified as lignocellulosic biomass, mainly comprised of hemicellulose, cellulose, and lignin. As reported in the literatures, hemicellulose degraded at a temperature of 220–315 °C, and cellulose with crystalline structure decomposed at a higher temperature range of 280–380 °C[38]. Due to the cross-linked phenolic structure, lignin degraded over a wide temperature range (160–900 °C) at a very slow rate[38]. Therefore, the sharp peak shown in second region with a peak temperature of 320 °C was mainly attributed to the degradation of cellulose, the shoulder on the left of this peak (~300 °C) was mainly because of hemicellulose decomposition, and the big tail of the peak (380–550 °C) was mainly caused by the lignin degradation. Fig. 4(b) showed the TG and DTG curves of pyrolysis of waste tire at various heating rates. The slight weight loss (9.9%) occurred prior to 300 °C is probably caused by the release of moisture, oil, plasticizer and additives in waste tire, which was reported by others[13,25,28]. Over 50% weight loss took place between 300 °C and 500 °C with two apparent degradation peaks, primarily corresponding to the decomposition of rubbers in waste tire including both NR and synthetic rubbers (SR). Cui et al.[39] investigated the thermal decomposition behaviors of NR, BR, SBR, and their mixtures, and found NR decomposed at around 385 °C, SBR decomposed at higher temperature of 465 °C, and the decomposition of BR contributed one major peak 466 °C and a tiny peak at 380 °C, respectively. However, the decomposition temperatures of rubbers can be affected by the content of vulcanizing agents in waste tire. Higher vulcanization leads to more stable structure, therefore higher decomposition temperature[34]. Thus, the peak at 370 °C shown in Fig. 4(b) was mainly attributed to the decomposition of NR. The peak at 420 °C was mainly associated with the decomposition of both BR and SBR. Similar results were also reported by others[25,26,28]. The peak showed after 600 °C was probably caused by the decomposition of some inorganic substances in waste tire[34].

The TG and DTG results obtained from the co-pyrolysis of corn stover and waste tire with the mass ratio of 1:1 were presented in Fig. 4(c). The overall process can be divided into three stages. The first stage was before 150 °C, corresponding to the release of moisture and small volatiles. The second stage (150–500 °C) was considered the active pyrolysis stage with 56.27% weight loss. According to the discussions on individual feedstock pyrolysis above, the second stage mainly involved the degradation of major components of biomass and waste tire (i.e. hemicellulose, cellulose, lignin, NR, BR, and SBR). The decomposition temperature of each component overlapped, forming a DTG curves with three pronounced peaks. The last stage (> 500 °C) was mainly associated with the degradation of carbonaceous materials in the char residues and inorganic substances in waste tire. The plateaued TG curve after 700 °C indicated the completion of the co-pyrolysis process with a final residue of 37.2%, which was due to the unreacted fixed carbon and ash.

For both pyrolysis of individual feedstock and co-pyrolysis, heating rates did not significantly affect the shape of TG and DTG curves and the weight of pyrolysis final residues. As the heating rate increased from 5 °C/min to 20 °C/min, the temperature gradient and difference between the outside and inner core of the feedstock increased[40]. Therefore, the heat transfer resistance increased with increasing heating rates, leading to a shift of the TG and DTG curves to a higher temperature side at higher heating rates. Similar behavior has also been reported in the literatures[24,41,42].

To further illuminate the possible synergistic effects occurred during degradation for co-pyrolysis of corn stover and waste tire, the mass loss difference between experimental and theoretical values ΔW was defined as below:

$$\Delta W = W_{exp} - (k_1 W_1 + k_2 W_2) \quad (15)$$

in which W_{exp} denotes the mass loss of co-pyrolysis process, W_1 and W_2 denote the mass losses of individual pyrolysis of corn stover and waste tire, and k_1 and k_2 denote respectively the initial mass fractions of corn stover and waste tire in co-pyrolysis. In this study, $k_1 = k_2 = 0.5$.

Positive ΔW means actual decomposition mass was greater than the theoretical values, indicating promoting effects occurred, while negative ΔW implies inhibiting effects occurred during co-pyrolysis.

Fig. 5 presents the variations of ΔW with degradation temperatures at heating rates of 5, 10, and 20 °C/min. For all heating rates, ΔW was not equal to zero at the temperature range of 150–800 °C, indicating interactions existed between corn stover and waste tire. The synergies between corn stover and waste tire were possibly caused by three aspects as follows: 1) soften tire could cover corn stover and thus inhibit evolution of volatiles; 2) soften tire as coatings could benefit the heat accumulation and promote the degradation of corn stover; and 3) initiation of tire pyrolysis could consume free radicals generated by corn stover and then suppressed pyrolysis of corn stover[43,44]. At the heating rates of 5 °C/min and 10 °C/min, ΔW was negative at all temperature and peaked at around 350 °C, indicating exhibitions of inhibitory effects in co-pyrolysis of corn stover and waste tire. At the heating rate of 20 °C/min, positive ΔW with a maximum value of 5% at temperature of 400 °C was observed, which implies there was positive synergy between two feedstocks. Xu et al.[45] also reported higher heating rate could enhance the promoting effects in co-pyrolysis of polyvinylidene fluoride and pine sawdust. Thus, more apparent positive synergistic effects could be observed in fast co-pyrolysis process that has much higher heating rates.

3.3. Fraser-Suzuki deconvolution

Co-pyrolysis of corn stover and waste tire is a complex process involving overlapping reactions. To better understand the kinetic behaviors, it is essential to apply deconvolution procedure to separate the global process into reactions of multiple pseudo-components. Deconvolution can be performed using symmetric functions (e.g. Gaussian, Lorentz, and Logistic) or asymmetric functions (e.g. Bi-Gaussian, Weibull, and Fraser-Suzuki). Fraser-Suzuki function with an asymmetric factor has been reported as an appropriate function to well fit the experimental data derived from thermal degradation of biomass and polymers[22,46,47]. In order to mitigate the inference of drying step, deconvolution was only applied to the process occurred after 150 °C here. According to the thermal degradation behaviors of corn stover and waste tire discussed above, in this study, the DTG curves of co-pyrolysis was deconvoluted into profiles of seven pseudo-components using Fraser-Suzuki functions. Three of them represented the major components of corn stover (i.e. hemicellulose, cellulose, and lignin), and four of them represented the main constituents in waste tire (i.e. additives, NR, SR, and inorganic substances). Fig. 6 shows the deconvoluted curves of seven pseudo-components at various heating rates. Comp 1 to Comp 7 respectively denotes additives, hemicellulose, cellulose, NR, SR, lignin, and inorganic substances. For all heating rates, modeling curves derived

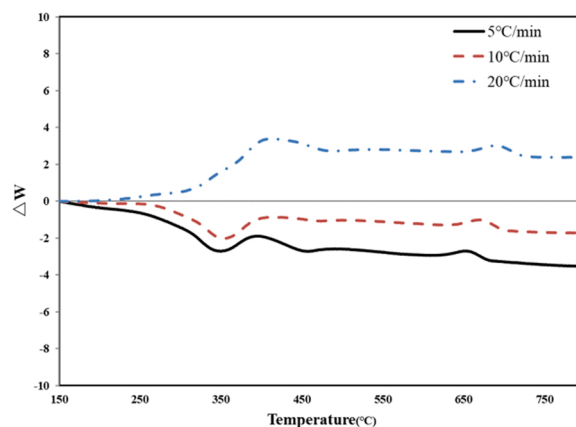


Fig. 5. Variations of ΔW with degradation temperatures at different heating rates.

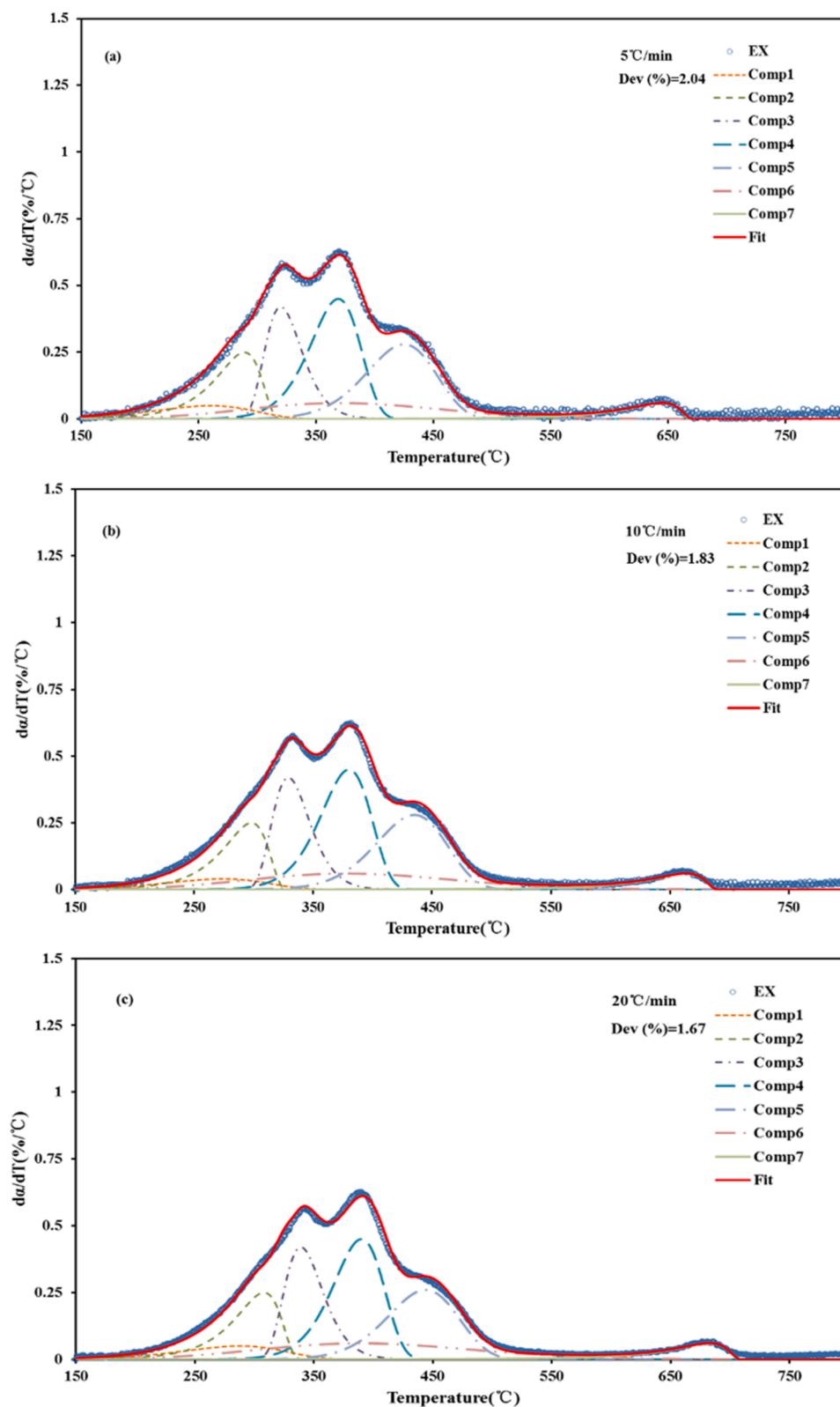


Fig. 6. Deconvoluted DTG curves at different heating rates: (a) 5 °C/min, (b) 10 °C/min, and (c) 20 °C/min.

from Fraser-Suzuki deconvolution had a good fit with the curves from experiments with small deviations ($\text{Dev}(\%) \leq 2$), indicating the rationality to adopt Fraser-Suzuki deconvolution results to further investigate the co-pyrolysis process kinetic features. Fraser-Suzuki deconvolution parameters of each pseudo-component are given in Table 2, and these parameters were primarily selected depending on the

pyrolysis characteristics of each component as discussed in Section 3.2. Peak height H_p reflects the component degradation rate. For all pseudo-components, H_p almost did not change with varied heat rates. The highest H_p was observed for Comp 4 (NR) followed by Comp 3 (cellulose), corresponding to the most apparent degradation peaks in

Table 2
Fraser-Suzuki deconvolution parameters.

β ($^{\circ}\text{C min}^{-1}$)		Comp1	Comp2	Comp3	Comp4	Comp5	Comp6	Comp7
5	H_p	0.05	0.25	0.42	0.45	0.28	0.06	0.06
	T_p	260.00	289.00	320.00	369.00	425.00	370.00	645.00
	W_{hf}	100.00	44.00	37.00	50.00	70.00	196.00	50.00
	A_s	-0.30	-0.60	0.30	-0.28	-0.20	0.10	-0.90
	C_i	5.27	13.26	17.08	24.63	21.16	12.55	4.27
10	H_p	0.04	0.25	0.42	0.45	0.28	0.06	0.06
	T_p	274.00	298.00	329.00	380.00	435.00	378.00	664.00
	W_{hf}	100.00	43.00	37.00	50.00	70.00	203.00	50.00
	A_s	-0.30	-0.60	0.30	-0.28	-0.20	0.10	-0.90
	C_i	4.27	12.98	17.08	24.63	21.16	12.99	4.27
20	H_p	0.05	0.25	0.42	0.45	0.26	0.06	0.06
	T_p	288.00	308.00	339.00	390.00	444.00	389.00	683.00
	W_{hf}	100.00	44.00	38.00	50.00	70.00	210.00	50.00
	A_s	-0.30	-0.60	0.30	-0.28	-0.18	0.10	-0.90
	C_i	5.40	13.29	17.54	24.63	19.6	13.44	4.27

co-pyrolysis process. T_p is the peak temperature, indicating the thermal stability of each pseudo-component. The thermal stability order of these pseudo-components is Comp 1 (additives) < Comp 2 (hemicellulose) < Comp 3 (cellulose) < Comp 4 (NR) < Comp 5 (lignin) < Comp 6 (SR) < Comp 7 (inorganic substances). Due to the heat and mass transfer limitation, T_p of each pseudo-component shifted to higher temperature as heating rates increased. The peak half-width W_{hf} , representing the pyrolysis temperature range. Lignin had the maximum value of W_{hf} because of its high thermal stability caused by complex cross-linked structure. A_s is the asymmetric factor. Heating rates did not significantly impact the trend of both W_{hf} and A_s . C_i represents the proportion of each-pseudo components. Corn stover was composed of about 26.49% hemicellulose, 33.63% cellulose, and 25.98% lignin, based on which the theoretical C_i values for hemicellulose, cellulose, and lignin in this study

are 13.24%, 16.82%, and 12.99%[48]. C_i values for pseudo-hemicellulose, pseudo-cellulose, and pseudo-lignin obtained from Fraser-Suzuki deconvolution were consistent with the theoretical values. In terms of the compositions of waste tire calculated from Fraser-Suzuki deconvolution, pseudo-NR had the highest proportion of 24.63% followed by SR. The compositions of tire varied greatly with different brands and different formula, however NR and SR were basically the two main ingredients, which agreed with the results obtained in this study[28].

3.4. Apparent activation energy estimation by isoconversional methods

Isoconversional method including KAS, FWO, and Friedman were applied to calculate the apparent activation energy of each pseudo-

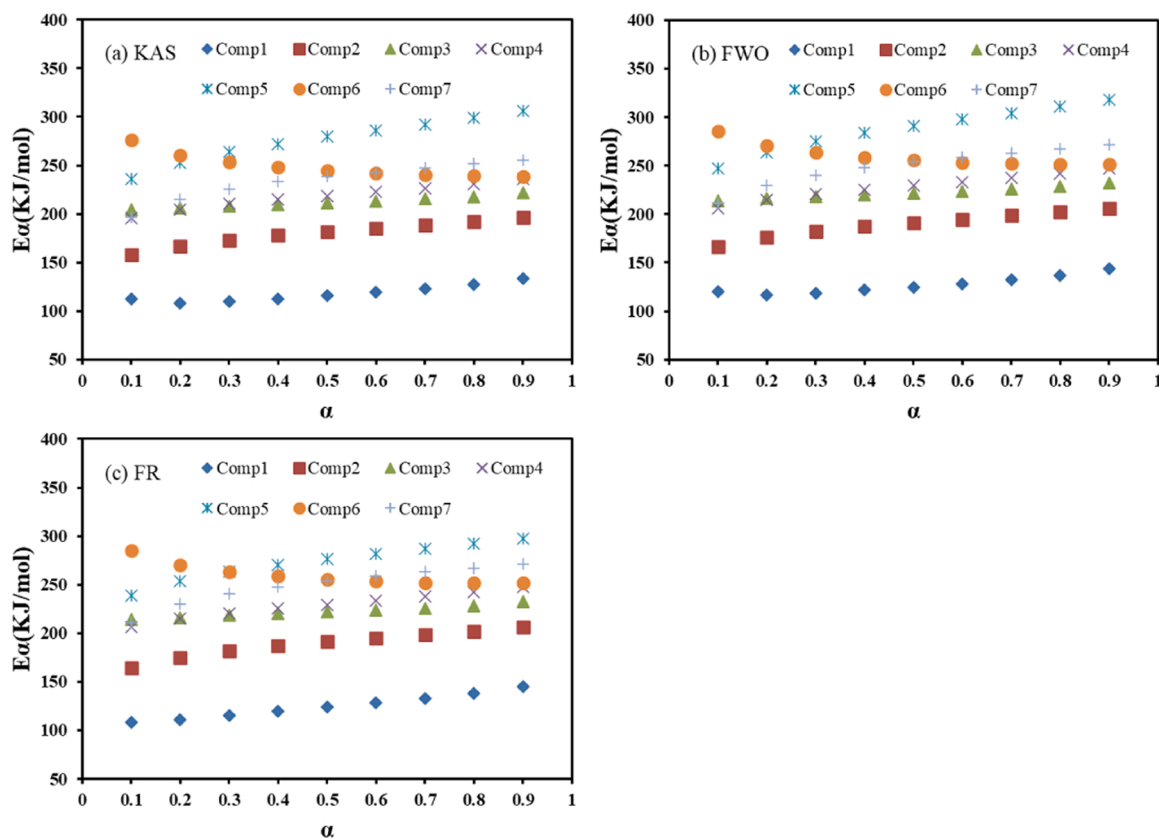


Fig. 7. The activation energy of each pseudo-component at different conversion rates calculated by three isoconversional methods: (a) KAS, (b) FWO, and (c) Friedman.

component obtained by Fraser-Suzuki deconvolution (Fig. S1-S7). For all cases, high correlation coefficients ($R^2 > 0.96$) were achieved (Table S5 in supplementary materials), implying the accuracy and reliability of the calculated activation energies. Fig. 7 presents the activation energies of seven pseudo-components calculated from three isoconversional methods and their changes with conversion rates. The activation energy value of each pseudo-component did not vary significantly with conversion rates with a deviation less than 20%, indicating that the degradation of each pseudo-component can be regarded as a single-step reaction and confirming the reasonability to deconvolute the corn stover and waste tire co-pyrolysis process using Fraser-Suzuki function [17]. Moreover, activation energy of each pseudo-component estimated by these three methods did not show significant differences. Similar results were also reported in literatures. Romero et al. [49] calculated the activation energy of three fractions of biomass using KAS, FWO and Friedman methods, and found that the activation energies obtained from these three methods did not differ significantly. Singh et al. [50] reported that activation energies of corn cob, PE and their blends calculated using KAS, FWO, starink, FR and Vyavkin methods did not have too many differences.

Comp 1 represents the additives in waste tire and showed the lowest activation energy (118.21–127.10 kJ/mol) due to its low thermal stability [25]. Comp 2 is associated with the degradation of hemicellulose and had a low activation energy of 180.32–189.58 kJ/mol. Hemicellulose is mainly composed of sugars with a rich branching structure, which makes it less thermally stable and requires less bonding energy to form the active state compounds. The activation energies of Comp 3 and Comp 6 were 212.21–222.32 kJ/mol and 249.41–260.43 kJ/mol, corresponding to the degradation of pseudo-cellulose and pseudo-lignin. Romero et al. [49] investigated the kinetics of three types of biomass using deconvolution method, and found activation energies for pseudo-hemicellulose, pseudo-cellulose, and pseudo-lignin were respectively in the range of 165.1–202.4 kJ/mol, 204.3–238.1 kJ/mol, and 214.5–245.0 kJ/mol, which agrees with the results obtained in this study. Comp 4 and Comp 5 represent the pyrolysis of NR and SR including BR and SBR with the activation energies of 217.89–228.64 kJ/mol and 273.29–288.16 kJ/mol, which are in consistent with the values reported in the literatures. Yang et al. [51] studied the kinetics of tire pyrolysis, and the calculated activation energy of NR was 207 kJ/mol and that of BR was 215 kJ/mol. Oh et al. [52] investigated the pyrolysis kinetics of SBR and the activation energy of

SBR was 238–241 kJ/mol. The order of activation energy for each pseudo-component was $\text{Comp5} > \text{Comp6} > \text{Comp7} > \text{Comp4} > \text{Comp3} > \text{Comp2} > \text{Comp1}$. Similar trend was also reported by others. Sharma et al. [24] reported that pseudo lignin had the highest activation energy (301.62–316.72 kJ/mol) followed by cellulose (162.90–165.67 kJ/mol) and hemicellulose (156.25–158.47 kJ/mol) when studied biomass pyrolysis kinetics. Rijo et al. [28] studied the kinetics of waste tire pyrolysis and showed that additives had lowest activation energy, and the activation energy of SBR was higher than that of NR.

3.5. Reaction model and pre-exponential factor determination

Fig. 8 compares the theoretical curves shown in Table S1 with the experimental values of each pseudo-component, and the reaction mechanism function for each pseudo-component can be determined. Comp1, Comp 3, Comp 4, Comp 5 and Comp 6 all followed the Order-based model with slight differences on the number of reaction order. Comp 2 followed the Geometrical contraction model (R3) and Comp 7 followed the Diffusion model (D2). Wang et al. [30] investigated the kinetics of co-pyrolysis of pine wood with waste plastics and showed that hemicellulose followed the Geometrical contraction model, while cellulose and lignin followed the Order-based model. Whilst Sharma et al. [24] found that the pyrolysis of pseudo-cellulose and hemicellulose followed a two-dimensional contraction zone reaction mechanism (R2) and a secondary reaction mechanism (O2), respectively. For lignin, no exact reaction mechanism was observed. Irmak et al. [53] reported that the reaction mechanism of waste tire pyrolysis belonged to the Order-based model with the number of orders between 3 and 4. The variances on the reaction mechanisms may be caused by the different materials and reaction conditions used in each study.

Based on the obtained reaction mechanism function and the activation energy derived from KAS method, pre-exponential factor of each pseudo-component was calculated using Eq. (9) and shown in Table 3. So far kinetic model of pyrolysis of each pseudo-component can be established by substituting the determined kinetic triplets (i.e. activation energy, pre-exponential factor, and reaction mechanism) into Eq. (4), which is the fundamental information needed for further optimization and scale-up of lignocellulosic biomass and waste tire co-pyrolysis process.

It is quite challenging to perform the kinetic analysis of overlapping

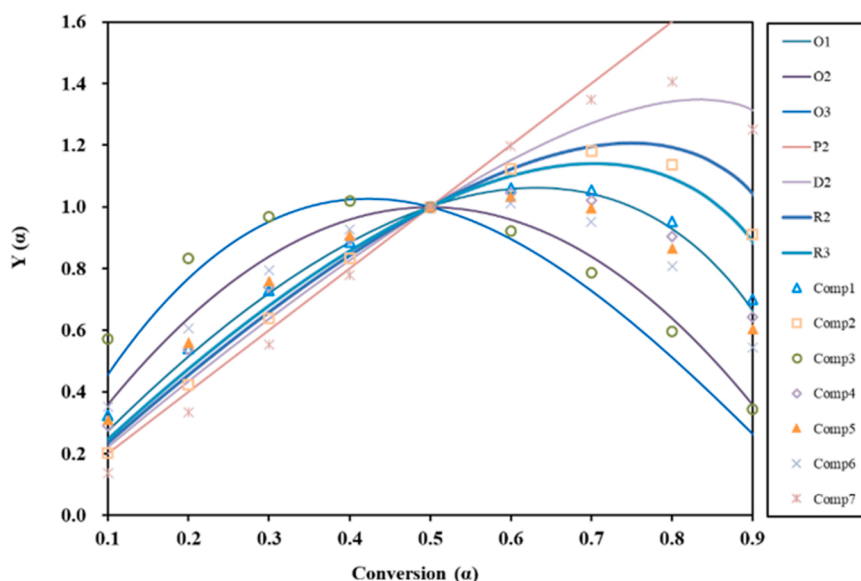


Fig. 8. Master plots of each pseudo component.

Table 3
Pre-exponential factor of each pseudo-component.

	Comp1	Comp2	Comp3	Comp4	Comp5	Comp6	Comp7
Pre-exponential factor (s^{-1})	1.85×10^8	1.16×10^{14}	3.49×10^{14}	1.22×10^{14}	2.25×10^{17}	1.24×10^{22}	1.81×10^{10}

multi-step reactions such as co-pyrolysis process of corn stover and waste tire due to its reaction diversity and complexity. As recommended by the International Confederation for Thermal Analysis and Calorimetry (ICTAC), Frazer-Suzuki function, a mathematical deconvolution method, was applied in this study, separating the global process into pseudo-reactions of seven major components of the feedstock. Though peak deconvolutions conducted here followed the pyrolysis characteristics of individual component strictly and the results greatly fitted the experimental data, Frazer-Suzuki function is still a mathematical approach disregarding any mutual dependence between the reactions of individual component. Its feasibility and accuracy highly depend on the knowledge of feedstock characteristics and chemical mechanisms of a process. Detailed characterizations of lignocellulosic biomass and tire samples, and extensive studies on pyrolysis behaviors of related model compounds would be potential future work to better understand the chemical mechanism of co-pyrolysis process and provide more fundamental information for kinetic analysis. Additionally, thermogravimetric measurements under a broad heating rate range and a wide variety of temperature programs combined with evolved gas analysis would be necessary to further validate or supplement the results obtained in this study.

4. Conclusion

In this study, pyrolysis and kinetic behaviors of co-pyrolysis of corn stover and waste tire were investigated. Pyrolysis product distribution analysis indicated that addition of waste tire into fast pyrolysis of biomass could promote the production of hydrocarbon compounds production. Thermogravimetric experiments were performed using the mixtures at heating rates of 5, 10 and 20 °C/min. Positive synergistic effects between corn stover and waste tire were observed at higher heating rate. Due to the complexity of the co-pyrolysis process, the DTG curve was divided into seven pseudo-components (i.e. pseudo-additives, hemicellulose, cellulose, lignin, NR, SR, and inorganic substances) using the Fraser-Suzuki deconvolution method for further kinetic analysis. The model obtained after deconvolution fitted well with the experimental data with a deviation of less than 2%. Seven pseudo-components were subjected to kinetic parameter calculations using the KAS, FWO and Friedman isoconversional methods. The results showed that the activation energies calculated by the three methods do not differ significantly. The activation energy of the pseudo-component is in the order of SR (273.29–288.16 kJ/mol) > lignin (249.41–260.43 kJ/mol) > inorganic substances (234.22–249.27 kJ/mol) > NR (217.89–228.64 kJ/mol) > cellulose (212.21–222.32 kJ/mol) > hemicellulose (180.32–189.58 kJ/mol) > additives (118.21–127.10 kJ/mol). The reaction mechanism of each pseudo-component was determined using the master plot method. Pseudo-additives, cellulose, NR, SR, and lignin all followed the Order-based model with slight differences on the number of reaction order. Hemicellulose followed the Geometrical contraction model (R3) and inorganic substances followed the Diffusion model (D2). The results of this study provide the theoretical basis for the practical application of co-pyrolysis process. However, future work on co-pyrolysis chemical mechanism study and thermogravimetric measurements under a broad condition would be essential to further validate or supplement results obtained in this study.

CRedit authorship contribution statement

Guanqun Luo: Conceptualization, Methodology, Writing – original draft, Writing – review & editing, Funding acquisition, Project

administration. **Weimin Wang:** Formal analysis, Visualization, Writing – original draft. **Wen Xie:** Formal analysis, Visualization. **Yuanjun Tang:** Methodology, Writing – review & editing, Funding acquisition. **Yousheng Xu:** Writing – review & editing, Funding acquisition. **Kaige Wang*:** Resources, Writing – review & editing, Funding acquisition, Project administration.

Declaration of Competing Interest

The authors declare the following financial interests/personal relationships which may be considered as potential competing interests: Guanqun Luo reports financial support was provided by National Natural Science Foundation of China. Yousheng Xu reports financial support was provided by National Natural Science Foundation of China. Kaige Wang reports financial support was provided by Zhejiang Provincial Natural Science Foundation. Yuanjun Tang reports financial support was provided by Zhejiang Provincial Natural Science Foundation.

Data Availability

No data was used for the research described in the article.

Acknowledgement

The authors would like to acknowledge the financial supports from the National Natural Science Foundation of China (Grant No. 52006196 and Grant No. 11972324) and the Zhejiang Provincial Natural Science Foundation, China (Grant No. LGG22E060004 and Grant No. LQ21E060001).

Appendix A. Supporting information

Supplementary data associated with this article can be found in the online version at [doi:10.1016/j.jaap.2022.105743](https://doi.org/10.1016/j.jaap.2022.105743).

References

- [1] H. Hassan, J.K. Lim, B.H. Hameed, Recent progress on biomass co-pyrolysis conversion into high-quality bio-oil, *Bioresour Technol* 221 (2016) 645–655.
- [2] A. Kumar, K. Kumar, N. Kaushik, S. Sharma, S. Mishra, Renewable energy in India: current status and future potentials, *Renew Sustain Energy Rev* 14 (8) (2010) 2434–2442.
- [3] J. Wang, Z. Zhong, K. Ding, B. Zhang, A. Deng, M. Min, et al., Co-pyrolysis of bamboo residual with waste tire over dual catalytic stage of CaO and co-modified HZSM-5, *Energy* 133 (2017) 90–98.
- [4] M. Guillain, K. Fairouz, S.R. Mar, F. Monique, L. Jacques, Attrition-free pyrolysis to produce bio-oil and char, *Bioresour Technol* 100 (2009) 6069–6075.
- [5] B. Zhang, Z. Zhong, K. Ding, Z. Song, Production of aromatic hydrocarbons from catalytic co-pyrolysis of biomass and high density polyethylene: analytical Py-GC/MS study, *Fuel* 139 (2015) 622–628.
- [6] K. Ding, A. He, D. Zhong, L. Fan, S. Liu, Y. Wang, et al., Improving hydrocarbon yield via catalytic fast co-pyrolysis of biomass and plastic over ceria and HZSM-5: an analytical pyrolyzer analysis, *Bioresour Technol* 268 (2018) 1–8.
- [7] F. Abnisa, Wan, W.M.A. Daud, A review on co-pyrolysis of biomass: an optional technique to obtain a high-grade pyrolysis oil, *Energy Convers Manag* 87 (2014) 71–85.
- [8] M. Singh, S.A. Salaudeen, B.H. Gilroyed, S.M. Al-Salem, A. Dutta, A review on co-pyrolysis of biomass with plastics and tires: recent progress, catalyst development, and scaling up potential, *Biomass Convers Biorefin* (2021).
- [9] M. Niu, R. Sun, K. Ding, H. Gu, X. Cui, L. Wang, et al., Synergistic effect on thermal behavior and product characteristics during co-pyrolysis of biomass and waste tire: influence of biomass species and waste blending ratios, *Energy* 240 (2022), 122808.
- [10] M.Z. Farooq, M. Zeeshan, S. Iqbal, N. Ahmed, S.A.Y. Shah, Influence of waste tire addition on wheat straw pyrolysis yield and oil quality, *Energy* 144 (2018) 200–206.

- [11] J.D. Martínez, J.D. Martínez, A. Veses, A.M. Mastral, R. Murillo, M.V. Navarro, et al., Co-pyrolysis of biomass with waste tyres: upgrading of liquid bio-fuel, *Fuel Process Technol.* 119 (2014) 263–271.
- [12] Q. Cao, J. Li-e, W. Bao, Y. Lv, Investigations into the characteristics of oils produced from co-pyrolysis of biomass and tire, *Fuel Process Technol.* 90 (2009) 337–342.
- [13] D.Y.C. Leung, C. Wang, Kinetic study of scrap tyre pyrolysis and combustion, *J Anal Appl Pyrolysis* 45 (1998) 153–169.
- [14] X. Cheng, P. Song, X. Zhao, Z. Peng, S. Wang, Liquefaction of ground tire rubber at low temperature, *Waste Manag* 71 (2018) 301–310.
- [15] P. Lahijani, Z.A. Zainal, A.R. Mohamed, M. Mohammadi, Co-gasification of tire and biomass for enhancement of tire-char reactivity in CO₂ gasification process, *Bioresour Technol* 138 (2013) 124–130.
- [16] K.W. Chew, S.R. Chia, W.Y. Chia, W.Y. Cheah, H.S.H. Munawaroh, W.J. Ong, Abatement of hazardous materials and biomass waste via pyrolysis and co-pyrolysis for environmental sustainability and circular economy, *Environ Pollut* 278 (2021), 116836.
- [17] S. Vyazovkin, A.K. Burnham, J.M. Criado, L.A. Pérez-Maqueda, C. Popescu, N. Sbirrazzuoli, ICTAC kinetics committee recommendations for performing kinetic computations on thermal analysis data, *Thermochim Acta* 520 (2011) 1–19.
- [18] N. Söyler, S. Ceylan, Thermokinetic analysis and product characterization of waste tire-hazelnut shell co-pyrolysis: TG-FTIR and fixed bed reactor study, *J Environ Chem Eng* 9 (2021), 106165.
- [19] S. Rasam, A. Moshfegh Haghighi, K. Azizi, A. Soria-Verdugo, M. Keshavarz Moraveji, Thermal behavior, thermodynamics and kinetics of co-pyrolysis of binary and ternary mixtures of biomass through thermogravimetric analysis, *Fuel* 280 (2020), 118665.
- [20] K. Azizi, A. Moshfegh Haghighi, M. Keshavarz Moraveji, M. Olazar, G. Lopez, Co-pyrolysis of binary and ternary mixtures of microalgae, wood and waste tires through TGA, *Renew Energy* (2019).
- [21] A. Anca-Couce, A. Berger, N. Zobel, How to determine consistent biomass pyrolysis kinetics in a parallel reaction scheme, *Fuel* 123 (2014) 230–240.
- [22] M. Hu, Z. Chen, S. Wang, D. Guo, C. Ma, Y. Zhou, et al., Thermogravimetric kinetics of lignocellulosic biomass slow pyrolysis using distributed activation energy model, Fraser-Suzuki deconvolution, and iso-conversional method, *Energy Convers. Manag* 118 (2016) 1–11.
- [23] X. Wang, M.H. Hu, W. Hu, Z. Chen, S. Liu, Z. Hu, et al., Thermogravimetric kinetic study of agricultural residue biomass pyrolysis based on combined kinetics, *Bioresour Technol* 219 (2016) 510–520.
- [24] P. Sharma, O.P. Pandey, P.K. Diwan, Non-isothermal kinetics of pseudo-components of waste biomass, *Fuel* 253 (2019) 1149–1161.
- [25] D.Y.C. Leung, C.L. Wang, Kinetic modeling of scrap tire pyrolysis, *Energy Fuels* 13 (1999) 421–427.
- [26] A. Quek, Balasubramanian RJJohm, An algorithm for the kinetics of tire pyrolysis under different heating rates, *J Hazard Mater.* 166 (1) (2009) 126–132.
- [27] T. Menares, J. Herrera, R. Romero, P. Osorio, L.E. Arteaga-Pérez, Waste tires pyrolysis kinetics and reaction mechanisms explained by TGA and Py-GC/MS under kinetically-controlled regime, *Waste Manag* 102 (2020) 21–29.
- [28] B. Rijo, A.P. Soares Dias, L. Wojnicki, Catalyzed pyrolysis of scrap tires rubber, *J Environ Chem Eng* 10 (1) (2022), 107037.
- [29] G. Lopez, R. Aguado, M. Olazar, M. Arabiourrutia, J. Bilbao, Kinetics of scrap tyre pyrolysis under vacuum conditions, *Waste Manag* 29 (10) (2009) 2649–2655.
- [30] W. Wang, G. Luo, Y. Zhao, Y. Tang, K. Wang, X. Li, et al., Kinetic and thermodynamic analyses of co-pyrolysis of pine wood and polyethylene plastic based on Fraser-Suzuki deconvolution procedure, *Fuel* 322 (2022), 124200.
- [31] A. Ephraim, V. Pozzobon, D. Lebonnois, C. Peregrina, P.J. Sharrock, A. Nzihou, et al., Pyrolysis of wood and PVC mixtures: thermal behaviour and kinetic modelling, *Biomass Convers Biorefin* (2020) 1–15.
- [32] Y. Wen, I.N. Zaini, S. Wang, W. Mu, P.G. Jönsson, W. Yang, Synergistic effect of the co-pyrolysis of cardboard and polyethylene: A kinetic and thermodynamic study, *Energy* 229 (2021), 120693.
- [33] H. Xie, Q. Yu, Q. Qin, H. Zhang, P. Li, Study on pyrolysis characteristics and kinetics of biomass and its components, *J. Renew. Sustain. Energy* 5 (2013), 013122.
- [34] X. Tang, Z.-S. Chen, J. Liu, Z. Chen, W. Xie, F. Evrendilek, et al., Dynamic pyrolysis behaviors, products, and mechanisms of waste rubber and polyurethane bicycle tires, *J Hazard Mater* 402 (2020), 123516.
- [35] L. Wang, M. Chai, R. Liu, J. Cai, Synergetic effects during co-pyrolysis of biomass and waste tire: a study on product distribution and reaction kinetics, *Bioresour Technol* 268 (2018) 363–370.
- [36] H. Zhang, R. Xiao, J. Nie, B. Jin, S. Shao, G. Xiao, Catalytic pyrolysis of black-liquor lignin by co-feeding with different plastics in a fluidized bed reactor, *Bioresour Technol* 192 (2015) 68–74.
- [37] P. Duan, B. Jin, Y. Xu, F. Wang, Co-pyrolysis of microalgae and waste rubber tire in supercritical ethanol, *Chem Eng J* 269 (2015) 262–271.
- [38] H. Yang, R. Yan, H. Chen, D.H. Lee, C. Zheng, Characteristics of hemicellulose, cellulose and lignin pyrolysis, *Fuel* 86 (12–13) (2007) 1781–1788.
- [39] H. Cui, J. Yang, Z. Liu, Thermogravimetric analysis of two Chinese used tires, *Thermochim Acta* 333 (2) (1999) 173–175.
- [40] S. Maiti, S. Purakayastha, B. Ghosh, Thermal characterization of mustard straw and stalk in nitrogen at different heating rates, *Fuel* 86 (2007) 1513–1518.
- [41] G.K. Gupta, M.K. Mondal, Kinetics and thermodynamic analysis of maize cob pyrolysis for its bioenergy potential using thermogravimetric analyzer, *J Therm Anal Calor* 137 (4) (2019) 1431–1441.
- [42] S. Gupta, P. Mondal, Catalytic pyrolysis of pine needles with nickel doped gamma-alumina: Reaction kinetics, mechanism, thermodynamics and products analysis, *J Clean Prod* 286 (2021), 124930.
- [43] Q. Bu, K.-S. Chen, H.M. Morgan, J. Liang, X. Zhang, L. Yan, et al., Thermal behavior and kinetic study of the effects of zinc-modified biochar catalyst on lignin and low-density polyethylene (LDPE) co-pyrolysis, *Trans ASABE* 61 (2018) 1783–1793.
- [44] R. Chen, S. Zhang, K. Cong, Q. Li, Y. Zhang, Insight into synergistic effects of biomass-polypropylene co-pyrolysis using representative biomass constituents, *Bioresour. Technol.* 307 (2020), 123243.
- [45] Z. Xu, C. Zhang, Z.-X. He, Q. Wang, Pyrolysis characteristic and kinetics of polyvinylidene fluoride with and without Pine Sawdust, *J Anal Appl Pyrolysis* 123 (2017) 402–408.
- [46] A.O. Aboiyade, T. Hugo, M. Carrier, E.L. Meyer, R.G. Stahl, J.H. Knoetze, et al., Non-isothermal kinetic analysis of the devolatilization of corn cobs and sugar cane bagasse in an inert atmosphere, *Thermochim. Acta* 517 (2011) 81–89.
- [47] C. García-Garrido, P.E. Sánchez-Jiménez, L.A. Pérez-Maqueda, A. Perejón, J.M. Criado, Combined TGA-MS kinetic analysis of multistep processes. Thermal decomposition and ceramification of polysilazane and polysiloxane preceramic polymers, *Phys Chem Chem Phys* 42 (2016) 29348–29360.
- [48] L. Huang, T. Ding, R. Liu, J. Cai, Prediction of concentration profiles and theoretical yields in lignocellulosic biomass pyrolysis, *J Therm Anal Calor* 120 (2015) 1473–1482.
- [49] L.M. Romero Millán, F.E. Sierra Vargas, A. Nzihou, Kinetic analysis of tropical lignocellulosic agrowaste pyrolysis, *BioEnergy Res* 10 (2017) 832–845.
- [50] S. Singh, T. Patil, S.P. Tekade, M.B. Gawande, A.N. Sawarkar, Studies on individual pyrolysis and co-pyrolysis of corn cob and polyethylene: thermal degradation behavior, possible synergism, kinetics, and thermodynamic analysis, *Sci Total Environ* (2021) 783.
- [51] J. Yang, S. Kaliaguine, C. Roy, Improved quantitative determination of elastomers in tire rubber by kinetic simulation of DTG curves, *Rubber Chem Technol* 66 (1993) 213–229.
- [52] S.C. Oh, H.C. Jun, H.T. Kim, Thermogravimetric evaluation for pyrolysis kinetics of styrene-butadiene rubber, *J Chem Eng Jpn* 36 (2003) 1016–1022.
- [53] D. Irmak Aslan, P. Parthasarathy, J.L. Goldfarb, S. Ceylan, Pyrolysis reaction models of waste tires: application of Master-Plots method for energy conversion via devolatilization, *Waste Manag* 68 (2017) 405–411.